Title

TARGET FRAGMENT ANGUIAR DISTRIBUTIONS FROM THE INTERACTION OF 3.0 GeV AND 12.0 GeV 12C WITH 197Au AND 238U

Author

Morita, Y.

Publication Date

1981-11-01

LBL-13425 Revised
Preprint

Lawrence Berkeley Laboratory
UNIVERSITY OF CALIFORNIA

Submitted to Physical Review C

TARGET FRAGMENT ANGULAR DISTRIBUTIONS FROM THE INTERACTION OF 3.0 GeV and 12.0 GeV ^{12}C WITH ^{197}Au AND ^{238}U

Y. Morita, W. Loveland, P.L. McGaughey,
and G.T. Seaborg

November 1981

Prepared for the U.S. Department of Energy under Contract W-7405-ENG-48

DISCLAIMER

Target Fragment Angular Distributions from the Interaction of 3.0 GeV and 12.0 GeV ^{12}C with ^{197}Au and ^{238}U

Y. Morita, W. Loveland,* P. L. McGaughey, and G. T. Seaborg

Lawrence Berkeley Laboratory, University of California, Berkeley, California 94720

This work was supported by the Director, Office of Energy Research, Division of Nuclear Physics of the Office of High Energy and Nuclear Physics of the U. S. Department of Energy under Contract W-7405-ENG-48.

* Radiation Center, Oregon State University, Corvallis, OR 97331

Target fragment angular distributions from the interaction of 3.0 GeV and 12.0 GeV ^{12}C with ^{197}Au and ^{238}U

Y. Morita, W. Loveland*, P.L.McGaughey, and G.T.Seaborg

Lawrence Berkeley Laboratory, University of California, Berkeley, California 94720

ABSTRACT

Target fragment angular distributions have been measured using radioanalytical techniques for the interaction of 3.0 and 12.0 GeV ^{12}C with ^{197}Au and ^{238}U. For the reaction of 3.0 GeV ^{12}C ions with ^{197}Au and ^{238}U, angular distributions were obtained for eight different target fragments ($89 \leq A \leq 155$), and seven different target fragments ($43 \leq A \leq 149$), respectively. In the interaction of 12.0 GeV ^{12}C with ^{197}Au and ^{238}U, the angular distributions of six different target fragments ($43 \leq A \leq 155$) from each target were measured. All the fragments observed from ^{197}Au target fragmentation show forward peaked angular distributions; from ^{238}U target fragmentation, typical neutron-rich fission fragment nuclides show isotropic distributions in the laboratory system while the rest of the fragments show forward peaked distributions similar to those observed in ^{197}Au target fragmentation. The observed angular distributions are consistent with the values of previously measured F/B ratios and are compared with predictions of the intranuclear cascade model. The measured angular distributions are used to test the validity of two step vector model of high energy reactions.

Target Fragment Angular Distributions From the Interaction of 3.0 GeV and 12.0 GeV ^{12}C with ^{197}Au and ^{238}U

Y. Morita, W. Loveland, P.L.McGaughey and G.T.Seaborg

Lawrence Berkeley Laboratory, University of California, Berkeley, California 94720

KEY WORDS

Relativistic heavy ion reaction, target fragmentation, target fragment angular distributions for 3.0 GeV, 12.0 GeV ^{12}C + ^{197}Au, ^{238}U; two step vector model, intranuclear cascade model.

1. INTRODUCTION

Despite extensive studies of high energy heavy ion reactions, no clear understanding of the reaction mechanisms exists. This description is especially applicable to target fragmentation reactions, i.e., reactions in which the initial projectile-target interaction produces relatively large fragments of the original target nuclei,ranging in mass number from A=24 up to the target mass number. Numerous theoretical models for the interactions have been proposed [1,2,3] and have been compared to experimental data [4,5,6] characterizing target fragmentation. Modest success is achieved in predicting the yields of fragments of differing Z and A, but the recoil energy and spatial distribution of the fragments are poorly described. Because of the importance of the fragment angular distributions in defining the operating reaction mechanisms, and because previous experimental studies of the kinematics of heavy ion-induced target fragmentation[5,7,8] have only involved measurements of F/B, a crude range-weighted measure of the extent of forward peaking of the angular distributions, we thought it to be of interest to directly measure the target frag-

ment angular distributions for relativistic heavy ion (RHI) reactions. In this paper, we report the first such measurements for relativistic nucleus-nucleus collisions.

The results were obtained from the interaction of a "sub-relativistic" heavy ion, 3.0 GeV ^{12}C, and a relativistic heavy ion, 12.0 GeV ^{12}C, with a very fissionable target nuclide, ^{238}U, and a much less fissionable heavy nuclide, ^{197}Au. Because of the extremely low intensity of the projectile beams ($< 10^{10}$ particles/minute) from the LBL Bevalac where this study was carried out, we were able to measure only crude four-point angular distributions for eight product nuclides from the interaction of 3.0 GeV $^{12}C + ^{197}Au$, seven from 3.0 GeV $^{12}C + ^{238}U$, six from 12.0 GeV $^{12}C + ^{197}Au$ and six from 12.0 GeV $^{12}C + ^{238}U$.

Nonetheless, certain interesting physical insights can be obtained from examining the results of these measurements.

2. EXPERIMENTAL

The major barrier to the measurement of target fragment angular distributions at the LBL Bevalac is the relatively low beam intensities. For the measurements described herein, ^{197}Au and ^{238}U target assemblies were placed behind one another in an evacuated beam tube ($P \sim 3 \times 10^{-2}$ torr). The attenuation and scattering of the beam in passing through the thin targets and catcher assemblies were negligible. No corrections were made for the effect of secondary particle induced reactions. The total particle fluence for the 3.0 GeV ^{12}C bombardment was 8.39×10^{13} particles delivered over a time of 1605 minutes, while the fluence for the 12.0 GeV ^{12}C bombardment was 9.07×10^{12} particles over a time period of 687 minutes. The Bevalac beam diameter during these irradiations was larger than the area of the target, resulting in a uniform ex-

posure of the entire target area. To overcome the problem of low beam intensity, special target-catcher assemblies were employed as shown in Fig.1. Each assembly consisted of 17 identical target foils, each surrounded by a conical catcher foil assembly in which the fragments recoiling from the target were stopped. Each ^{238}U target foil consisted of a 12.8 mg/cm^2 Al foil onto which a circular spot (1.59 cm diameter) of UF_4 of thickness 1.25 mg/cm^2 had been evaporated. Each ^{197}Au target consisted of 34.4 mg/cm Mylar foil with a similar circular spot of evaporated Au of thickness 1.00 mg/cm^2. Each catcher was a cone of height 0.84 cm and with a radius at the base of 3.86 cm. The catcher assemblies were constructed of Mylar of thickness 7.32mg/cm^2; like the target backing foils, these catchers should have been sufficiently thick to stop the recoiling target fragments.[5,8,9,10] After irradiation, each conical catcher foil was cut into four pieces, corresponding to angular ranges of 0°-30°, 30°-50°, 50°- 70°and 70°-90°, with respect to the beam direction through the center of the evaporated target. Catcher foils corresponding to the same angular range from each of the 17 targets were combined and counted as a single sample using a Ge(Li) detector. Gamma-ray spectroscopic techniques that have been generally described elsewhere[11], were used to assay the relative amounts of different radionuclides present in each foil.

The determination of the effective solid angle subtended by each catcher foil, the correction for fragment absorption and scattering in the relatively thick target, and the correction for widely differing counting efficiencies due to the extended counting sources produced in this work were complex matters. First, the relative solid angles subtended by the various catcher conic sections with respect to the extended area of circular targets were numerically evaluated. As part of this procedure, the average recoil angles of

the fragments stopped in the different catcher foil sections were evaluated. The average angles corresponding to the four pieces of conical catcher were 22.7°, 33.1°, 44.3°, and 73.8°.

The next step involved the use of a single identical $^{238}UF_4$ target-catcher assembly to measure the fission fragment angular distribution from the 43.0 MeV helium-ion -induced fission of ^{238}U. During this bombardment, the helium ion beam from the LBL 88-inch cyclotron was defocused to uniformly irradiate the entire 1.6 cm diameter ^{238}U target, thus simulating the conditions present in the Bevalac experiments. The relative activities of typical fission products in the four pieces of the conical catcher assembly were assayed using the same counting geometry and techniques as employed in the Bevalac experiments. Relative values of the differential cross sections, $d\sigma/d\Omega(\theta)$, were calculated for each fission fragment radionuclide using the measured activities and the numerically calculated solid angles. The values of $d\sigma/d\Omega(\theta)$ for the different nuclides were then averaged and compared to the known gross fission fragment angular distribution,[12] for this reaction. This comparison was used to generate a set of correction factors for the effects of extended counting sources and fission fragment absorption in the target material. The correction factors obtained from this calibration were 1.00, 1.03, 1.04, 1.44 for the different catcher foils corresponding to the average angles 22.7°, 33.1°, 44.3°, 73.8°, respectively.

Strictly speaking, this calibration procedure should be only valid for fragments from the helium-ion-induced fission of ^{238}U. However, since the fragments from RHI-induced fission are thought to have energies similar to those of fragments from low energy helium-ion-induced fission, our calibration procedure should be adequate for fission fragments. Also, since many non-

fission products (with $50 \leq A \leq 140$) from relativistic heavy ion (RHI) reactions with ^{197}Au and ^{238}U have ranges similar to the fission fragments;[5,9] the errors involved in our procedure should also be acceptable. The lightest fragments ($A \leq 50$) from RHI reactions have ranges[5,8,9] in matter that exceed fission fragment ranges by factors of up to 4 or 5. No attempt was made to correct for this difference between the light fragments and the fission fragments. The problem of how to evaluate the absorption and scattering of the heavy fragments ($A \geq 140$) produced in RHI reactions is more serious. For example, fragments with $A > 165$ produced in these reactions are estimated to have ranges[5,8,9] in the target material of $\leq 2 mg/cm^2$, meaning that a significant number of fragments with large recoil angles were stopped in the target. Therefore, while it was possible to measure angular distributions for such fragments, the fission fragment calibration procedures are grossly inadequate for such fragments. We will only consider the angular distributions of fragments with $A < 150$ whose ranges in matter are at least twice the target thickness.

3. RESULTS AND DISCUSSION

The measured fragment angular distributions for reaction of 3.0 GeV ^{12}C with ^{197}Au and ^{238}U and the reaction of 12.0 GeV ^{12}C with ^{197}Au and ^{238}U are shown in Figures 2, 3, 4 and 5, respectively, and are also tabulated in Tables I,II,III and IV. The uncertainties in $d\sigma/d\Omega(\theta)$ in these figures and tables only reflect the uncertainties due to counting statistics and do not reflect any evaluation of systematic errors. Despite the measures used to overcome the problems of low beam intensity, an appreciable uncertainty is present in some of the data. Nonetheless, there are many interesting qualitative trends apparent in the results. In general,one observes roughly isotropic angular

distributions for neutron-rich fragments generally considered to be ^{238}U fission products, such as ^{97}Zr, ^{99}Mo and ^{133}I (Figures 3 and 5), in good agreement with previous determinations[13,14,15] that the RHI-induced fission of ^{238}U which leads to the formation of neutron-rich fission products is a low excitation energy process resulting from peripheral collisions with low momentum transfer. In the case of ^{238}U, the fragments other than neutron-rich fission products show forward-peaked distributions with the greatest degree of forward-peaking being observed in the ^{149}Gd angular distribution. This is in qualitative agreement with the trends of F/B ratios[5] observed for the reaction of 4.8 GeV ^{12}C with ^{238}U. For the interactions of RHI's with ^{197}Au, all the observed distributions are forward-peaked with a large degree of forward peaking observed for fragments with $145 \leq A \leq 155$, in agreement with general trends previously observed[9] in the F/B ratios for interactions of RHI's with ^{197}Au.

It is interesting to compare the fragment angular distributions measured in this work with similar data for the interaction of high energy protons with ^{238}U. Fortney and Porile[16] have measured the angular distribution of ^{48}Sc fragments in the interactions of 3.0 and 11.5 GeV protons with ^{238}U. They have observed a dramatic change with increasing proton energy in the character of the ^{48}Sc angular distributions with the distribution drifting from a forward-peaked distribution in the 3.0 GeV p + ^{238}U reaction to a sidewise peaked distribution in the 11.5 GeV p + ^{238}U reaction. A representation of these results is shown in Figures 3a and 5a, along with the distributions obtained in this work for ^{43}K. Although the uncertainties in the angular distributions from the RHI reactions are large, there is no evidence for this transition in our measurements.

One important reason for directly measuring the fission fragment angular distributions is to study the reaction kinematics in a model-independent way, unlike the use of the thick target-thick catcher recoil technique whose results are dependent upon the validity of the two step vector model.[17,18,19,20] In Fig. 3, we compare, for selected fragments, the angular distributions measured in this work with those deduced from a two step vector model analysis of thick target-thick catcher recoil data[21] for the reaction of 3.0 GeV ^{12}C with ^{238}U.

In these calculations of the fragment angular distributions, the values of the longitudinal component of the momentum imparted to the target fragment in the first step of the reaction, $P_{\parallel}$, for the fragment precursors as deduced in the two step vector model[20] analysis of thick target-thick catcher recoil data[21] were added vectorially to a series of isotropic momentum kicks corresponding to the momentum <P> given to the fragment during its de-excitation. <P> was chosen in accord with the results of the two step vector model analysis. No attempt was made to "smear out" the results of the calculation to simulate the effects of the finite angular resolution in the experimental data. For the one light nuclide, ^{43}K, and the typical fission product nuclides, the agreement between the measured and predicted angular distributions seems acceptable, especially in view of the finite angular resolution in the experimental measurements. This agreement is consistent with the continued use of this simple model to deduce crude information about average fragment momenta and energies for target fragmentation reactions in this energy region, although more sophisticated experiments[22] have indicated that some classes of events in reactions with similar projectile and targets are not consistent with the idea of two separable stages of the reaction.

It is of further interest to compare the simple single fragment angular distributions measured in this work with current theoretical models of nucleus-nucleus collisions. In Fig.4, we compare the measured ^{155}Dy angular distribution with that predicted for the A=155 fragments by the intranuclear cascade model of Yariv and Fraenkel [3] and a simple fragment de-excitation model for the reaction of 12.0 GeV ^{12}C with ^{197}Au. In the calculation of the final fragment angular distributions, the momentum-angle distributions of the A=155 fragment precursors were calculated using the intranuclear cascade model and these distributions were "smeared out" by vectorially adding to them a series of isotropic momentum kicks corresponding to the momentum <P> given to the fragment in its de-excitation. The values of <P> were chosen from the analysis of 4.8 GeV ^{12}C + ^{197}Au recoil data [9] assuming that <P> is relatively insensitive to changes in projectile energy. We assumed that each evaporated nucleon removed ~10 MeV from the precursor in deciding which precursor fragments contributed to the yield of the A=155 final fragments.

Upon examining Fig.4, one concludes that the intranuclear cascade model grossly underestimates the target fragment anisotropy in the interaction of 12.0 GeV ^{12}C with ^{197}Au. This is interesting because it has been shown previously [5] that the same model overestimates the fragment anisotropy in the interaction of 4.8 GeV ^{12}C with ^{238}U. Thus it might appear that the intranuclear cascade model gives the wrong energy dependence of the target fragment anisotropy in relativistic nucleus-nucleus collisions. In fact, this model predicts that the A=155 fragments should be preferentially emitted backwards (in the laboratory system) in the reaction of 25.2 GeV ^{12}C with ^{197}Au, a prediction not born out by observation.[9]

4. CONCLUSIONS

What new things have we learned as the result of these studies? They are:

1. It is possible, albeit marginal, to measure target fragment angular distributions in relativistic nucleus-nucleus collisions. To obtain a sufficient improvement in the quality of the experimental data (better angular resolution, thinner targets, less uncertainty) to allow detailed comparisons with similar data from proton-nucleus collisions will require 2-3 orders of magnitude more intense beams.

2. The magnitude of the fragment anisotropies and the variation of this anisotropy with fragment mass number is in general agreement with that which one would deduce from a two step vector model treatment of thick target-thick catcher recoil data. While more sophisticated experiments may offer more insight into the validity of this model, there is nothing in the angular distribution data that would indicate that use of this crude model to deduce average fragment energies and momenta and their trends in relativistic nucleus-nucleus collisions will lead to erroneous conclusions.

3. The comparison between the measured angular distributions and those calculated using the intranuclear cascade model (with a simple de-excitation model) revealed that the model fails to reproduce the experimental dependence of fragment anisotropy upon projectile energy. In the higher projectile energy reaction sampled in this work, the model underestimated the heavy fragment anisotropy, while previous studies at lower projectile energies showed the model to overestimate the heavy fragment anisotropy.

ACKNOWLEDGMENTS

We wish to thank the staff of the LBL Bevalac for the assistance in the performance of this experiment and T. Gee for making the Au and UF_4 targets. We are also grateful for the support of the people in our group.

This work was supported by the Director, Office of Energy Research, Division of Nuclear Physics of the Office of High Energy and Nuclear Physics of the U.S. Department of Energy under Contract W-7405-ENG-48.

REFERENCES

* Radiation Center, Oregon State University, Corvallis OR 97331

1. J. D. Bowman, W. J. Swiatecki, and C. F. Tsang; Lawrence Berkeley Laboratory Report No. LBL-2908 (1973).

2. W. D. Myers, Nucl. Phys. A296, 177 (1978).

3. Y. Yariv and Z. Fraenkel, Phys. Rev. C20, 2227 (1979).

4. D. J. Morrissey, W. R. Marsh, R. J. Otto, W. Loveland, and G. T. Seaborg, Phys. Rev. C18, 1267 (1978).

5. W. Loveland, Cheng Luo, P. L. McGaughey, D. J. Morrissey, and G. T. Seaborg, Phys. Rev. C24, 464 (1981).

6. P. L. McGaughey, D. J. Morrissey and G. T. Seaborg, Lawrence Berkeley Laboratory Report No. LBL-11588, p. 159.

7. W. Loveland, D. J. Morrissey, K. Aleklett, G. T. Seaborg, S. B. Kaufman, E. P. Steinberg, B. D. Wilkins, J. B. Cumming, P. E. Haustein, and H. C. Hseuh, Phys. Rev. C23, 253 (1981).

8. J. C. Cumming, P. E. Haustein, and H. C. Hseuh, Phys. Rev. C18, 1372 (1978).

9. S. B. Kaufman, E. P. Steinberg, B. D. Wilkins, and D. J. Henderson, Phys. Rev. C22, 1897 (1980).

10. L. C. Northcliffe and R. F. Schilling, Nucl. Data A7, 233 (1970).

11. D. J. Morrissey, D. Lee, R. J. Otto, and G. T. Seaborg, Nucl. Instr. Meth. 158, 499 (1979).

12. R. Vandenbosch, H. Warhanek, and J. R. Huizenga, Phys. Rev. 124, 846 (1961).

13. W. Loveland, R. I. Otto, D. J. Morrissey, and G. T. Seaborg, Phys. Rev. Lett. 39, 320 (1977).

14. R. H. Kraus, Jr., Oregon State University Nuclear Chemistry Progress Report 1979, DOE/ER/70035-1, p. 76.

15. W. G. Meyer, H. H. Gutbrod, Ch. Lukner, and A. Sandoval, Phys. Rev. C22, 179 (1980).

16. D. R. Fortney, and N. T. Porile, Phys. Lett. 76B, 553 (1978).

17. N. Sugarman, M. Campos, and K. Wielgoz, Phys. Rev. 101, 388 (1956).

18. N. T. Porile and N. Sugarman, Phys. Rev. 107, 1410 (1957).

19. N. Sugarman, H. Munzel, J. A. Panontin, K. Wielgoz, M. V. Ramaniah, G. Lange, and E. Lopez-Menchero, Phys. Rev. 143, 952 (1966).

20. L. Winsberg, Nucl. Instr. Meth. 150, 465 (1978).

References (cont.)

21. P. Johnson, W. Loveland, P. L. McGaughey, and G. T. Seaborg (to be published).

22. H. Wieman, A. Baden, M. Freedman, H. H. Gutbrod, D. J. Henderson, S. B. Kaufman, M. Maier, J. Peter, H. G. Ritter, E. P. Steinberg, H. Stelzer, A. I. Warwick, F. Weik, and B. D. Wilkins, Bull. Am. Phys. Soc. 26, 1111 (1981).

FIGURE CAPTIONS

Figure 1. Schematic drawing of target assembly showing use of seventeen identical target - conical catcher foil assemblies. XBL 8110-1479.

Figure 2. Target fragment angular distributions from the reaction of 3.0 GeV ^{12}C + ^{197}Au. XBL 8110-1480.

Figure 3. TArget fragment angular distributions from the reaction of 3.0 GeV ^{12}C + ^{238}U. The dashed curves are the results of computations using the two step vector model. The ^{48}Sc angular distribution (solid curve) from the reaction of 3.0 GeV p with ^{238}U (Ref. 16) is shown for comparison with the ^{43}K. XBL 8110-1481.

Figure 4. Target fragment angular distributions from the reaction of 12.0 GeV ^{12}C + ^{197}Au. The dashed curve is the result of calculations using the intranuclear cascade model. XBL 8110-1482.

Figure 5. Target fragment angular distributions from the reaction of 12.0 GeV ^{12}C + ^{238}U. The ^{48}Sc angular distribution (solid curve) from the reaction of 11.5 GeV p with ^{238}U (Ref. 16) is shown for comparison with the ^{43}K distribution. XBL 8110-1483.

TABLE I

Target Fragment Angular Distributions from the Reaction of 3.0 GeV ^{12}C with ^{197}Au

$\frac{d\sigma}{d\Omega}(\theta)$ (arbitrary units)

$\langle\theta_{LAB}\rangle$

Nuclide	23°	33°	44°	74°
^{89}Zr	2.25±0.27	1.31±0.09	1.06±0.05	1.±0.04
^{90}Nb	2.49±0.18	1.77±0.09	1.55±0.05	1.±0.03
^{97}Ru	3.13±0.20	1.53±0.13	2.08±0.06	1.±0.05
^{123}I	4.04±0.16	2.27±0.07	2.24±0.03	1.±0.02
^{145}Eu	6.26±0.37	5.19±0.26	3.19±0.15	1.±0.07
^{149}Gd	6.17±0.21	4.06±0.11	3.48±0.05	1.±0.05
^{152}Tb	4.28±0.31	3.68±0.16	2.80±0.08	1.±0.05
^{155}Dy	7.00±0.28	5.82±0.19	4.14±0.09	1.±0.05

TABLE II

Target Fragment Angular Distributions for the Reaction of 3.0 GeV with ^{238}U

$\frac{d\sigma}{d\Omega}(\theta)$ (arbitrary units)

$\langle\theta_{LAB}\rangle$

Nuclide	23°	33°	44°	74°
^{43}K	1.15±0.11	0.94±0.05	1.08±0.03	1.±0.03
^{72}As	1.13±0.20	0.89±0.09	1.01±0.08	1.±0.09
^{89}Zr	0.80±0.17	0.66±0.07	0.77±0.05	1.±0.05
^{97}Zr	0.84±0.10	0.80±0.04	0.96±0.03	1.±0.04
^{99}Mo	1.05±0.02	0.88±0.01	1.04±0.01	1.±0.01
^{133}I	1.13±0.12	0.89±0.01	1.04±0.04	1.±0.05
^{149}Gd	2.34±0.28	1.73±0.13	1.68±0.07	1.±0.08

TABLE III

Target Fragment Angular Distributions for the Reaction of 12.0 GeV ^{12}C with ^{197}Au

$\frac{d\sigma}{d\Omega}(\theta)$ (arbitrary units)

$\langle\theta_{LAB}\rangle$

Nuclide	23°	33°	44°	74°
^{89}Zr	2.78±0.72	2.78±0.50	0.67±0.17	1.±0.22
^{90}Nb	3.21±0.50	3.03±0.35	1.54±0.15	1.±0.14
^{97}Ru	2.15±0.53	1.29±0.21	1.26±0.11	1.±0.13
^{145}Eu	4.29±1.14	2.29±0.43	1.14±0.29	1.±0.14
^{149}Gd	9.33±1.58	3.00±0.58	1.67±0.25	1.±0.33
^{155}Dy	9.60±2.26	5.15±0.58	2.77±0.31	1.±0.27

TABLE IV

Target Fragment Angular Distributions for the Reaction of 12.0 GeV ^{12}C with ^{238}U

$\frac{d\sigma}{d\Omega}(\theta)$(arbitrary units)

$\langle\theta_{LAB}\rangle$

Nuclide	23°	33°	44°	74°
^{43}K	1.97±0.31	0.85±0.13	1.02±0.07	1.±0.10
^{72}As	2.80±0.78	0.71±0.16	0.75±0.14	1.±0.16
^{97}Zr	1.86±0.30	0.81±0.14	1.18±0.09	1.±0.10
^{99}Mo	1.12±0.12	0.96±0.05	1.15±0.03	1.±0.02
^{133}I	1.16±0.27	0.68±0.14	0.61±0.08	1.±0.13
^{149}Gd	5.67±1.56	4.78±1.22	1.22±0.22	1.±0.33

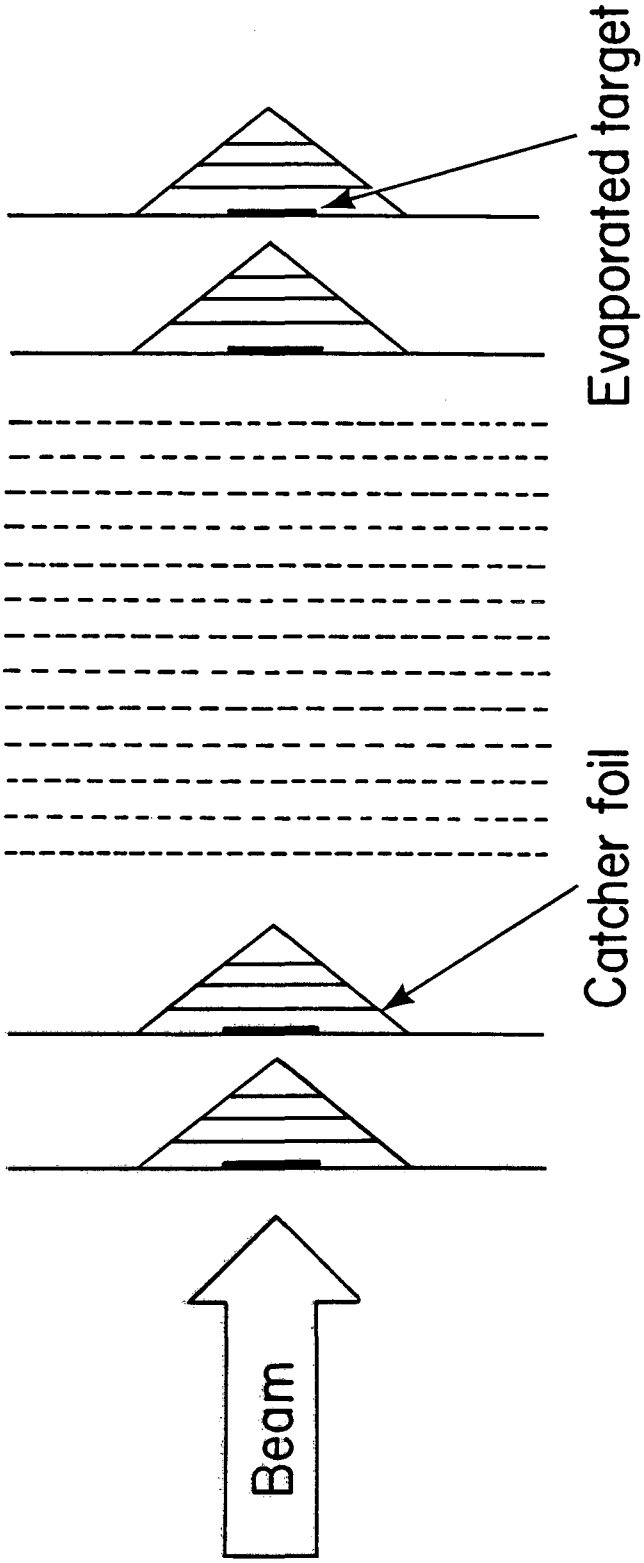

XBL 8110-1479

Figure 1

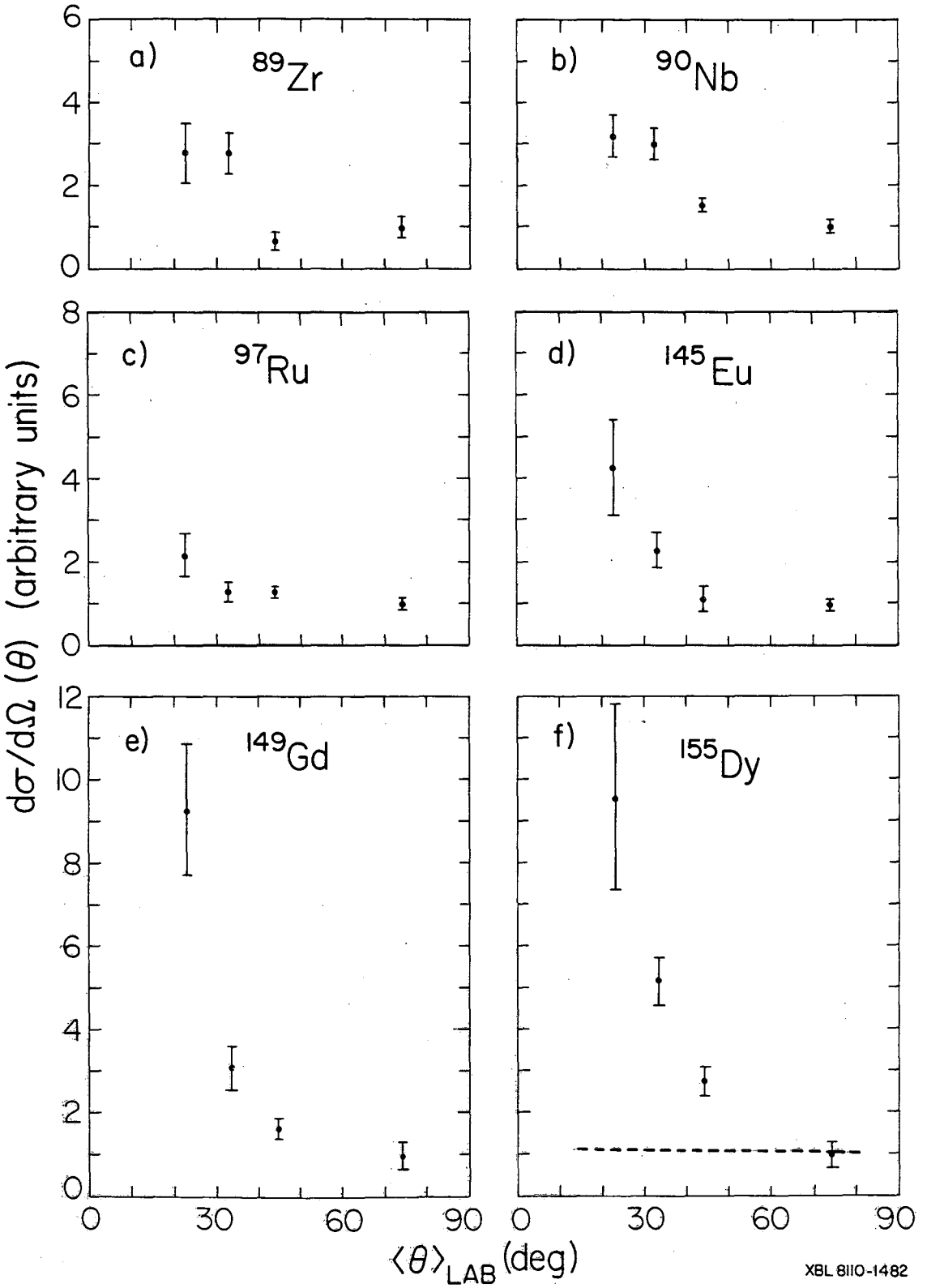
a) ^{89}Zr
b) ^{90}Nb
c) ^{97}Ru
d) ^{145}Eu
e) ^{149}Gd
f) ^{155}Dy
dσ/dΩ (θ) (arbitrary units)
⟨θ⟩LAB (deg)
0
30
60
90
XBL 8110-1482

Figure 2

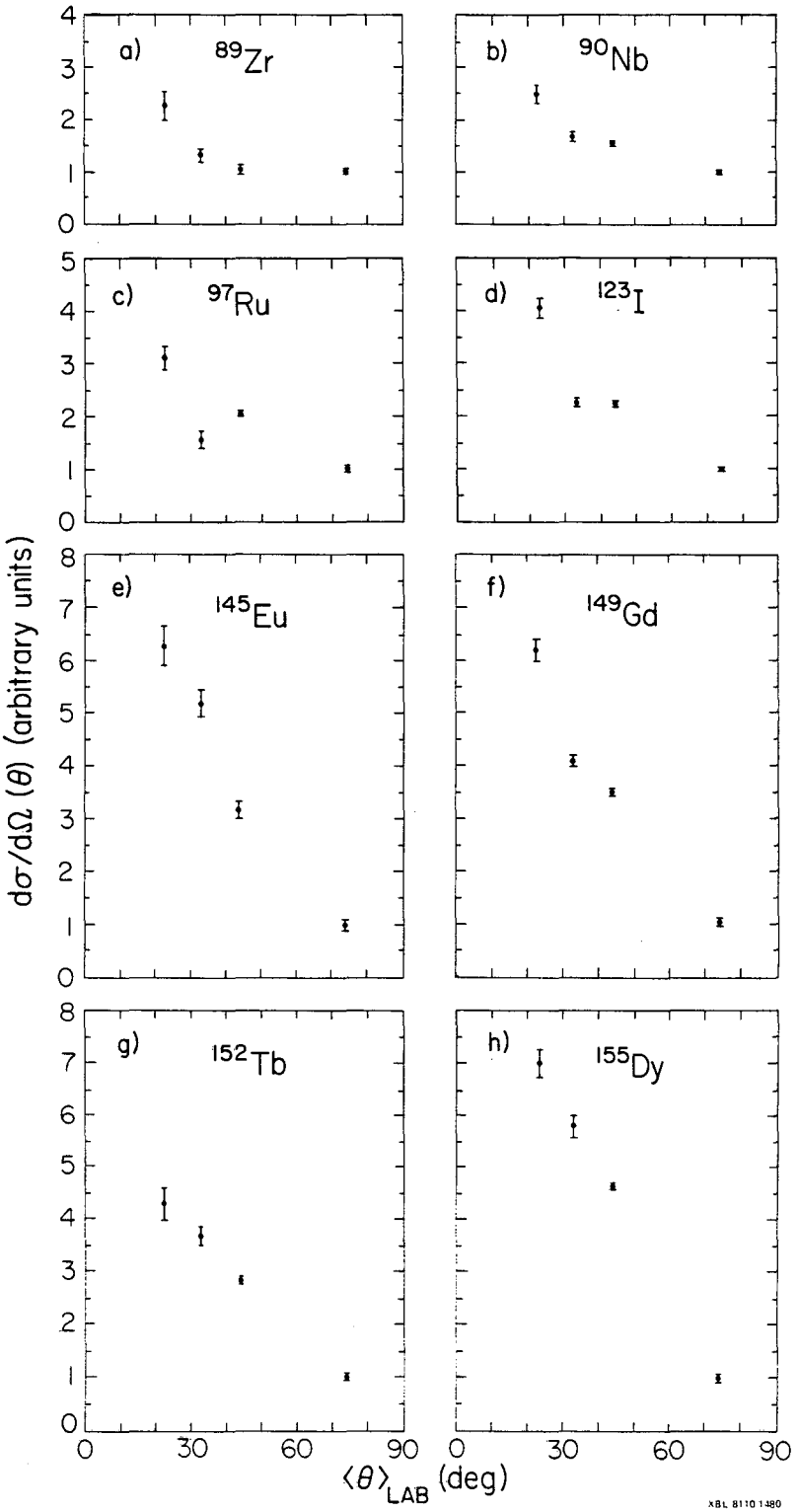
a) ^{89}Zr
b) ^{90}Nb
c) ^{97}Ru
d) ^{123}I
e) ^{145}Eu
f) ^{149}Gd
g) ^{152}Tb
h) ^{155}Dy
dσ/dΩ (θ) (arbitrary units)
⟨θ⟩$_{LAB}$ (deg)
0
30
60
90
XBL 8110 1480

Figure 3

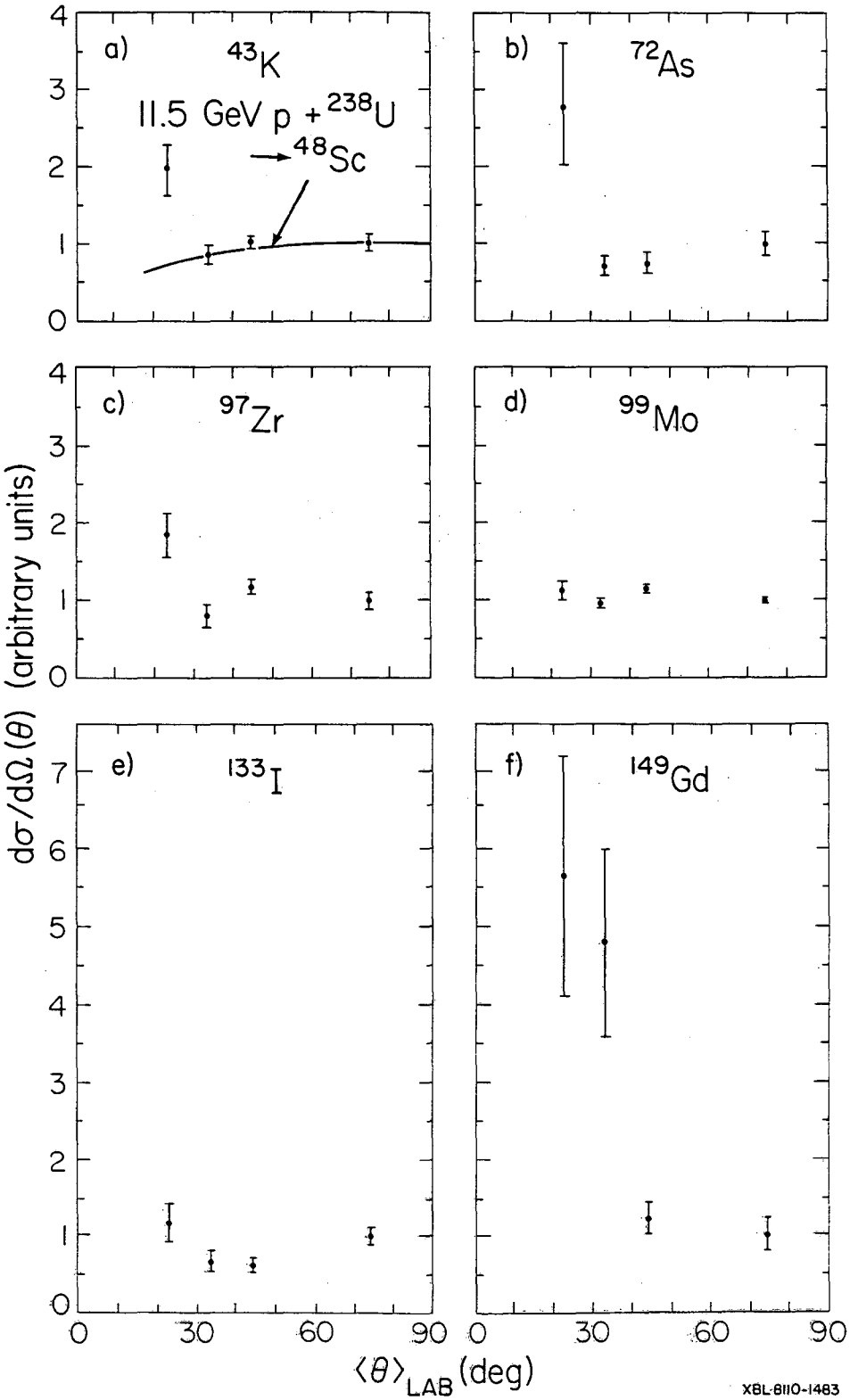
a) ^{43}K
11.5 GeV p + ^{238}U
^{48}Sc
b) ^{72}As
c) ^{97}Zr
d) ^{99}Mo
e) ^{133}I
f) ^{149}Gd
dσ/dΩ (θ) (arbitrary units)
⟨θ⟩$_{LAB}$ (deg)
0
30
60
90
XBL-8110-1483

Figure 4

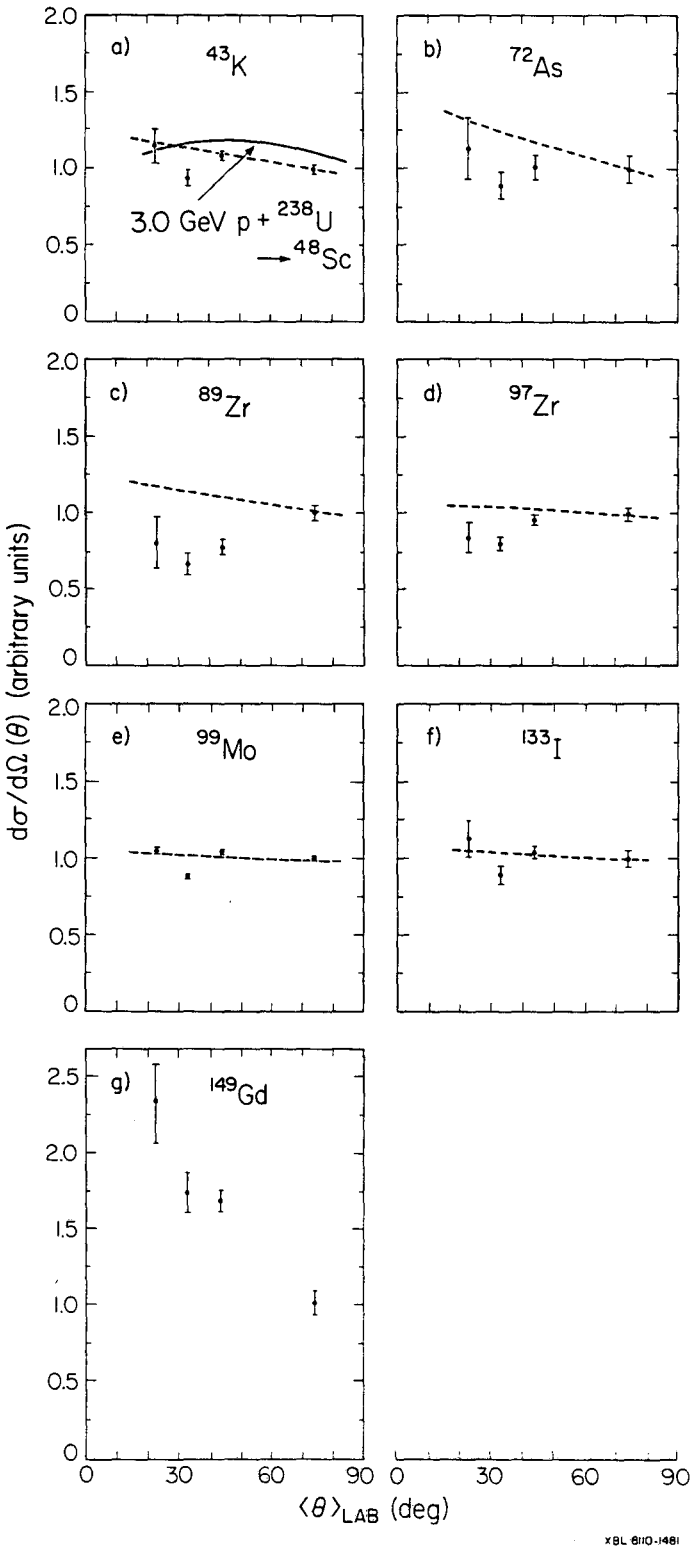
a) ^{43}K
3.0 GeV p + ^{238}U
→ ^{48}Sc
b) ^{72}As
c) ^{89}Zr
d) ^{97}Zr
e) ^{99}Mo
f) ^{133}I
g) ^{149}Gd
dσ/dΩ (θ) (arbitrary units)
⟨θ⟩$_{LAB}$ (deg)
XBL 8110-1481

Figure 5

TECHNICAL INFORMATION DEPARTMENT
LAWRENCE BERKELEY LABORATORY
UNIVERSITY OF CALIFORNIA
BERKELEY, CALIFORNIA 94720